Available online at www.sciencedirect.com
SCIENCE DIRECT
Thermochimica Acta 435 (2005) 129–134
thermochimica acta
www.elsevier.com/locate/tca

Glass transition behavior and crystallization kinetics of $Cu_{0.3}(SSe_{20})_{0.7}$ chalcogenide glass

A.A. Soliman *

Physics Department, Faculty of Science, Ain Shams University, Abbassia-11566, Cairo, Egypt

Received 20 December 2004; received in revised form 23 March 2005; accepted 4 May 2005
Available online 16 June 2005

Abstract

The glass transition behavior and crystallization kinetics of $Cu_{0.3}(SSe_{20})_{0.7}$ chalcogenide glass were investigated using differential scanning calorimetry (DSC), X-ray diffraction (XRD). Two crystalline phases (SSe_{20} and Cu_2Se) were identified after annealing the glass at 773 K for 24 h. The activation energy of the glass transition (E_g), the activation energy of crystallization (E_c), the Avrami exponent (n) and the dimensionality of growth (m) were determined. Results indicate that this glass crystallizes by a two-stage bulk crystallization process upon heating. The first transformation, in which SSe_{20} precipitates from the amorphous matrix with a three-dimensional crystal growth. The second transformation, in which the residual amorphous phase transforms into Cu_2Se compound with a two-dimensional crystal growth.

Keywords: Chalcogenide glasses; DSC; Glass transition; Crystallization kinetics

1. Introduction

The chalcogenide vitreous semiconductors (ChVS) have attracted much attention in the field of photo-induced effects since they exhibit photo-stimulated diffusion of metals (mainly Ag or Cu) into ChVS, which are applicable in a variety of microelectronics, optical memory, holography, diffractive optics and photoresistors [1]. These materials must be stable in the amorphous state at low temperature and have a short crystallization time [2]. Therefore, it is very important to know the glass forming ability and chemical durability of this type of materials.

Recently, I have paid much attention to evaluate the level of glass thermal stability for the investigated chalcogenide glass [1] and the determination of the critical radius of crystal nuclei for the two formed SSe_{20} and Cu_2Se phases and their dependence on different heating rates [3].

In the present work, the DSC traces at different heating rates ranging from 2 to 30 K/min are used for calculating the apparent activation energies of glass transition and crystallization.

2. Experimental

The $Cu_{0.3}(SSe_{20})_{0.7}$ chalcogenide glass was prepared by the quenching technique. Materials (99.999% pure) from Aldrich Chemicals Ltd. were weighted according to their atomic percentage and were sealed in a silica ampoule (length 15 cm, internal diameter 8 mm) with a vacuum $\sim 10^{-3}$ Pa. The ampoule was kept in a furnace and heated up to 1223 K at a rate of 4–5 K/min. After that ampoule was rocked frequently for 4 h at the maximum temperature to make the melt homogeneous. Quenching was done in ice-water. The amorphous nature and purity of prepared material was checked by X-ray diffraction (XRD) using X-ray diffractometer (Philips X'pert) in the range 19–90 in 0.03° 2θ steps with a counting time of 15 per step with Cu Kα radiation with graphite monochromator in the diffracted beam. Differential scanning calorimetry (DSC) experiments presented in this paper were performed using a Shimadzu DSC-50 instrument on

* Tel.: +202 4090262; fax: +202 6842123.
E-mail address: alaa_soliman2000@hotmail.com.

0040-6031/$ – see front matter © 2005 Elsevier B.V. All rights reserved.
doi:10.1016/j.tca.2005.05.008

samples of ≈15 mg (particle size around 40 μm) encapsulated in conventional platinum sample pans in an atmosphere of dry nitrogen at a flow of 30 ml/min. The instrument was calibrated with In, Pb, and Zn standards. The calorimetric sensitivity was 10 μW cm^{-1} and the temperature precision was ±0.1 K. Non-isothermal DSC curves were obtained with selected heating rates 2–30 K/min in the range 300–873 K. The values of the glass transition temperature (T_g), the onset temperature of crystallization (T_{ci}), the peak temperature of crystallization (T_{pi}) and the melting temperature (T_m) were determined by using the microprocessor of the apparatus.

3. Results and discussion

Fig. 1 gives typical continuous DSC traces obtained for $Cu_{0.3}(SSe_{20})_{0.7}$ chalcogenide glass at various heating rates of 2, 5, 10, 15, 20, 25 and 30 K/min. All the DSC traces exhibit the endothermic characteristic of a glass transition followed by two exothermic crystallization peaks at higher temperatures, indicating that the $Cu_{0.3}(SSe_{20})_{0.7}$ chalcogenide glass has a wide supercooled liquid region $\Delta T_i = T_{ci} - T_g$ and undergoes a two-stage crystallization process upon heating. The glass transition temperature (T_g) and the onset temperatures of crystallization (T_{ci}) have been defined as temperatures corresponding to the intersection of two linear portions adjoining the transition elbow of the DSC trace in the endothermic and exothermic directions [1]. The peak temperature of crystallization (T_{pi}) is the temperature at which the crystallization attains its maximum value and considered to be the peak temperature of the exothermic peak in DSC curve. The obtained parameters of T_g, T_{ci}, T_{pi} and ΔT_i are listed in Table 1. The Table reveals that these values are shifted to higher temperatures with increasing heating rate. Another interesting feature is that the intensity (i.e. peak height) and the area under the DSC traces increase with increasing heating rate (see Fig. 1). Fig. 2 exhibits that the endothermic broad peak of the $Cu_{0.3}(SSe_{20})_{0.7}$ chalcogenide glass shifts gradually to higher temperatures, the width of the supercooled liquid region increases with increasing heating rate, and the glass transition process is delayed to higher temperatures [4,5]. This phenomenon indicates that the glass transition as well as the crystallization behaves quite frequently in the literature [6–11].

Table 1
Transition temperatures of the $Cu_{0.3}(SSe_{20})_{0.7}$ chalcogenide glass

Temperature (K)	Heating rate α (K/min)						
	2	5	10	15	20	25	30
T_g	309.4	313.4	316.5	318.6	319.7	320.8	321.6
T_{c1}	342.0	348.1	352.9	356.6	359.1	360.3	361.9
T_{c2}	375.3	380.5	385.6	388.8	390.9	392.3	393.8
T_{p1}	349.8	356.7	362.5	357.7	370.9	371.7	374.3
T_{p2}	381.9	386.8	391.9	395.4	397.2	398.6	399.7
ΔT_1	32.6	34.7	36.4	38.0	39.4	39.5	40.3
ΔT_2	65.9	67.1	69.1	70.2	71.2	71.5	72.2

Three approaches are used for analyzing the dependence of T_g on the heating rate α. The first empirical relation has the following form [12]:

$$T_g = A + B \ln \alpha \quad (1)$$

where A and B are constants for a given composition and some particular temperature T. The constant B indicates the response of the configuration changes within the glass transition region to the heating rate. The plot of T_g versus $\ln \alpha$ for $Cu_{0.3}(SSe_{20})_{0.7}$ chalcogenide glass and fitting line with Eq. (1) are shown in Fig. 3(a). The good fitting result verifies that T_g can be well described by Lasocka's relationship. The calculated values of A and B are 306.2 and 4.5 K for the $Cu_{0.3}(SSe_{20})_{0.7}$ chalcogenide glass, respectively.

The second approach for analyzing T_g is based on the Kissinger's linear dependence [13] in the form:

$$\ln\left(\frac{\alpha}{T_g^2}\right) = -\frac{E_g}{RT} + \text{constant} \quad (2)$$

where E_g is the activation energy of glass transition for homogeneous crystallization with spherical nuclei and R

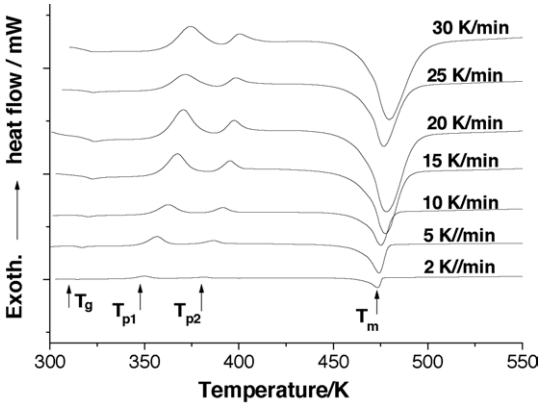

Fig. 1. DSC traces for the as-prepared $Cu_{0.3}(SSe_{20})_{0.7}$ chalcogenide glass at different heating rates.

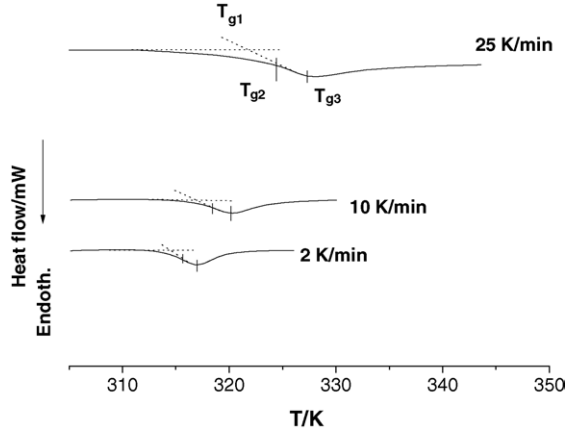

Fig. 2. DSC traces for $Cu_{0.3}(SSe_{20})_{0.7}$ chalcogenide glass showing the T_g dependence of the heating rate.

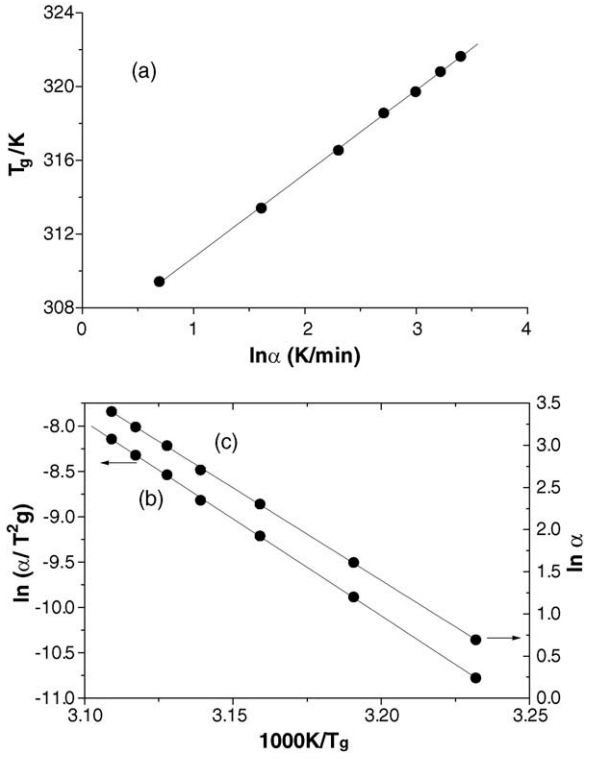

Fig. 3. (a) Plot of T_g vs. $\ln\alpha$ for $Cu_{0.3}(SSe_{20})_{0.7}$ chalcogenide glass, (b) plot of $\ln(\alpha/T_g^2)$ vs. $1000/T_g$ and (c) plot $\ln\alpha$ vs. $1000/T_g$ for $Cu_{0.3}(SSe_{20})_{0.7}$ chalcogenide glass.

is the universal gas constant. Fig. 3(b) shows the plot of $\ln(\alpha/T_g^2)$ versus $1000/T_g$ for the investigated glass. From the slope of the straight line, the value of E_g is equal to 177.93 ± 2.45 kJ/mol. Since the change of $\ln(T_g^2)$ with α is negligibly small compared with the change of $\ln\alpha$, then Eq. (2) can be simplified to:

$$\ln\alpha = -\frac{E_g}{RT_g} + \text{constant} \tag{3}$$

The relation between $\ln\alpha$ versus $1000/T_g$ is shown in Fig. 3(c). The calculated value of E_g for the $Cu_{0.3}(SSe_{20})_{0.7}$ chalcogenide glass is 182.91 ± 1.43 kJ/mol. Therefore, the average value of the activation energy of the glass transition is about 180.42 kJ/mol.

The third approach for analyzing T_g is based on the Moynihan et al. method [9–11]:

$$\frac{\mathrm{d}\ln|\alpha|}{\mathrm{d}\left(\frac{1}{T_g}\right)} = -\frac{E_g}{R} \tag{4}$$

For heating, Eq. (4) is applicable subject to the constraint that prior to heating the glassy material should be cooled from above to well bellow the glass transition region at a rate whose absolute value is equal to the rate of heating. T_g was determined for three characteristic points on each curve as shown in Fig. 2. The extrapolated onset of the heat capacity break (designated T_{g1}), the inflection point in the rapidly rising part of the heat capacity curve (designated T_{g2}), and the

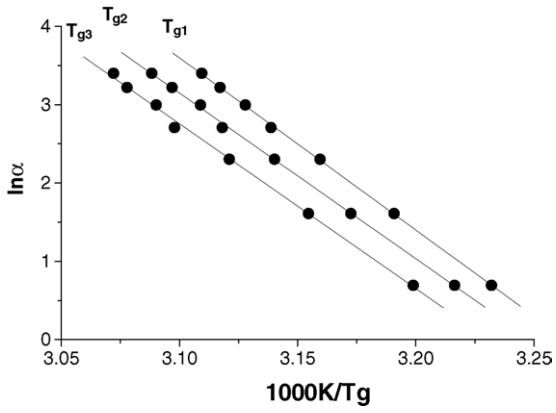

Fig. 4. $\ln\alpha$ vs. $1000/T_g$ plots for $Cu_{0.3}(SSe_{20})_{0.7}$ chalcogenide glass. The calculated E_g from the slopes is 177.85 kJ/mol.

heat capacity maximum (designated T_{g3}). Fig. 4 shows the plot of $\ln\alpha$ versus $1000/T_{g1}$, $1000/T_{g2}$ and $1000/T_{g3}$ for the $Cu_{0.3}(SSe_{20})_{0.7}$ chalcogenide glass. The three plots are linear and parallel within the scatter of the data. The calculated value of E_g is 177.85 ± 0.86 kJ/mol which agree very well with the value obtained by Kissinger method. The obtained value of the activation energy E_g for structural relaxation in the glass transition region determined via Eq. (4), along with values of T_g measured during heating at a rate between 2 and 30 K/min without cooling at a comparable rate. Moynihan et al. method showed that the glass activation energy, E_g does not change throughout the whole range of the glass transition region.

To determine the mechanism of crystallization from the DSC data the following equation given by Matusita et al. [14,15] has been used to obtain the Avrami exponent or order parameter, n and the dimensionality of growth, m.

$$\ln\left[-(1-\chi)\right] = -n\ln\alpha - \frac{1.052mE_c}{RT} + \text{constant} \tag{5}$$

where χ is the volume fraction of the crystal precipitated in the glass and heated at uniform rate, α is the uniform heating rate, E_c is the activation energy of the crystallization and R is the universal gas constant. To obtain n, $\ln[-\ln(1-\chi)]$ is plotted against $\ln\alpha$ at a fixed temperature. Fig. 5 shows such a plot for the two peaks of the $Cu_{0.3}(SSe_{20})_{0.7}$ chalcogenide glass at three different temperatures namely, 300, 305 and 310 K. The value of n has been evaluated from the slopes of the straight lines fit of these relations, and an average value of n was calculated to be 4.69 and 3.28 for the first and second crystallization peaks, respectively. For $Cu_{0.3}(SSe_{20})_{0.7}$ chalcogenide glass, no specific heat treatment was performed prior to the DSC scans to nucleate the sample. Therefore, n is considered to be equal to $(m+1)$ for the glass. The calculated values of n are not an integer, which means that the crystallization process of $Cu_{0.3}(SSe_{20})_{0.7}$ chalcogenide glass occurs with different mechanisms and the predominant one is the process in which $n=4$ for first peak and $n=3$ for the second peak [16,17]. Therefore, the value of the correspond-

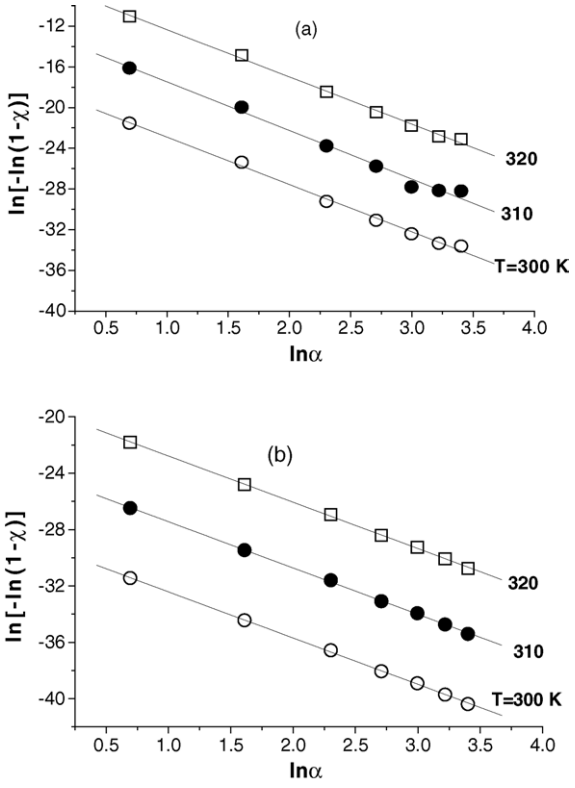

Fig. 5. Plot of $\ln[-\ln(1-\chi)]$ vs. $\ln\alpha$ at three different temperatures for (a) first peak and (b) second peak for $Cu_{0.3}(SSe_{20})_{0.7}$ chalcogenide glass.

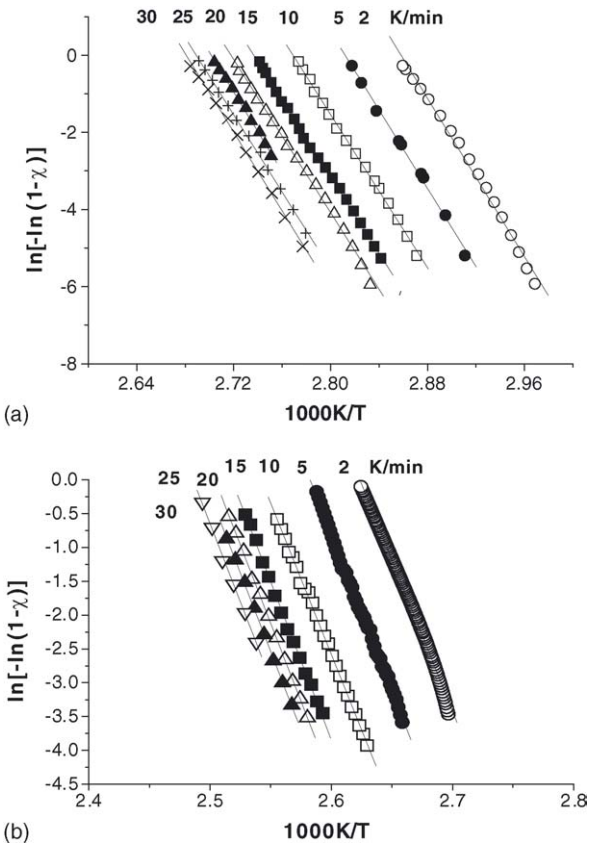

Fig. 6. Plot of $\ln[-\ln(1-\chi)]$ vs. $1000/T$ at three different temperatures for (a) first peak and (b) second peak for $Cu_{0..3}(SSe_{20})_{0.7}$ chalcogenide glass.

ing m is equal to 3 for first peak and $m = 2$ for the second one. Therefore, it is somewhat reasonable to suggest that the $Cu_{0.3}(SSe_{20})_{0.7}$ crystallization process can be carried out by a bulk crystallization in three and two dimensions for the first peak and second peak, respectively.

To determine mE_c at different heating rates, using the Matusita and Sakka equation (5), a graph of $\ln[-\ln(1-\chi)]$ versus $1000/T$ for the two crystallization peaks are plotted as shown in Fig. 6. The plots are found to be linear over most of the selected temperature range. Here, the analysis is restricted to the initial linear region which extends over a large temperature range [17].

The values of mE_c at different heating rates can be obtained from the slopes of Fig. 6 and seemed to be independent of the heating rate. Therefore, an average of mE_c were calculated by considering all the heating rates. The obtained mE_c values are 398.48 ± 5.71 and 365.58 ± 2.59 kJ/mol for the first and second crystallization peaks, respectively (see Table 2).

Knowing the crystallization mechanism, the activation energy for crystallization E_c can be obtained using the modified Kissinger expression [18].

$$\ln\left(\frac{\alpha^n}{T_p^2}\right) = -\frac{mE_c}{RT_p} + \ln K \tag{6}$$

where T_p is the peak crystallization temperature and K is a constant containing factors depending on the thermal history of the sample. The average values of n and m for the two crystallization peaks are used in Eq. (6) to plot the graph $\ln(\alpha/T_p^2)$ versus $1000/T_p$ (Fig. 7). From the slope of the graph E_c are found to be 175.47 ± 0.67 and 295.06 ± 0.66 kJ/mol for the first and second crystallization peaks, respectively (see Table 2). It is a common practice also to infer $(m/n)E_c$ from the slope of $\ln\alpha$ versus $1000/T_p$ plot itself. Fig. 7 shows the plot of $\ln\alpha$ versus $1000/T_p$ data for the $Cu_{0.3}(SSe_{20})_{0.7}$ chalcogenide glass. The value of $(m/n)E_c$ obtained from such a plot is listed in Table 2 for the two peaks.

Table 2
Data on n, m and E_c for the $Cu_{0.3}(SSe_{20})_{0.7}$ chalcogenide glass

Peak	From $\ln[-\ln(1-\chi)]$ vs. $1000/T$ and $\ln\alpha$ data				From $\ln(\alpha/T_p^2)$ vs. $1000/T_p$		From $\ln\alpha$ vs. $1000/T_p$	
	mE_c	n	m	E_c	$(m/n)E_c$	E_c	$(m/n)E_c$	E_c
First	398.48	4.68	3	132.83	112.48	175.47	118.05	184.16
Second	365.58	3.28	2	182.79	179.91	295.06	186.48	305.83

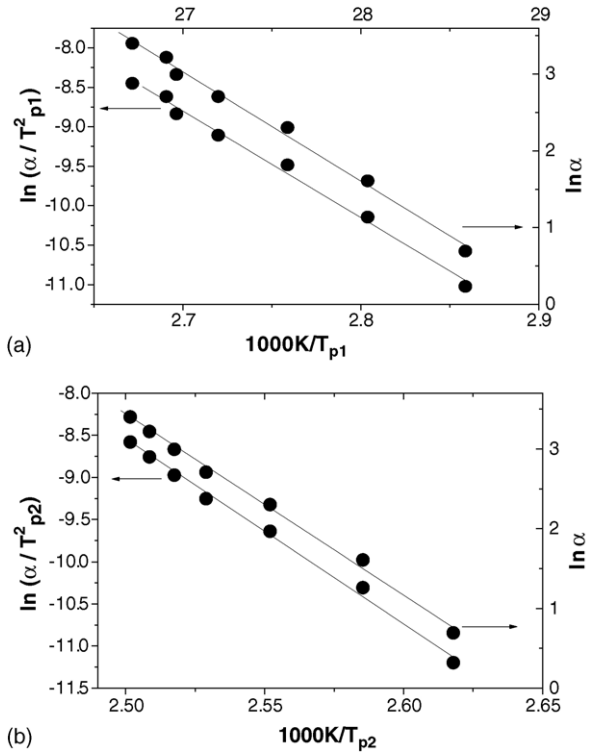

Fig. 7. Plot of $\ln(\alpha/T_p^2)$ and $\ln\alpha$ vs. $1000/T_p$ for (a) first and (b) second peaks for $Cu_{0.3}(SSe_{20})_{0.7}$ chalcogenide glass.

To further study the phase formation in process of crystallization, the investigated glass were annealed at an annealing temperature and then measured by DSC and standard XRD. Lasocka [12] suggested that the second glass transition can be clearly seen by crystallizing out the first glassy phase. By annealing the considered glass for 2 h at a temperature corresponding to the value of the peak crystallization temperature (T_{p1} = 362.5 K) of the first phase. Though most of the first crystallization exotherm is absent. Fig. 8 shows the continuous DSC traces at the heating rate of 10 K/min for as-prepared glass and annealed glass at 362.5 K for 2 h. The

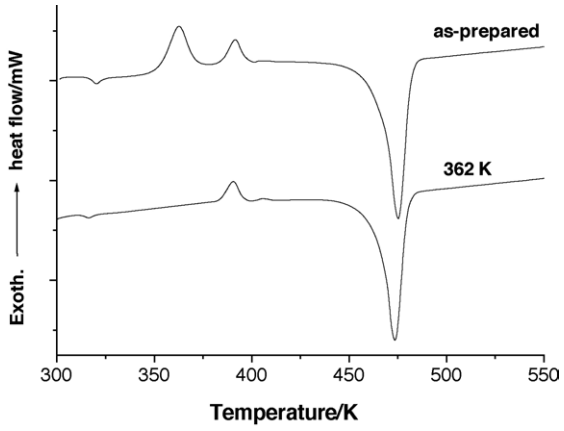

Fig. 8. DSC traces for the as-prepared $Cu_{0.3}(SSe_{20})_{0.7}$ chalcogenide glass and sample annealed at 362.5 K for 2 h. The heating rate is 10 K/min.

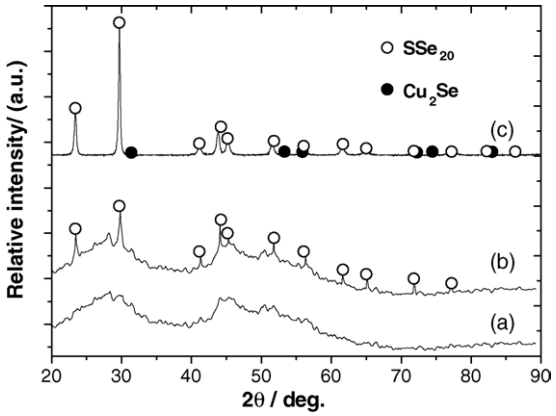

Fig. 9. X-ray diffraction patterns recorded at room temperature using Philips X' pert diffractometer with Cu Kα radiation for the as-prepared $Cu_{0.3}(SSe_{20})_{0.7}$ chalcogenide glass (a) and the sample annealed at 362 K for 2 h (b) and 773 K for 24 h.

annealing induces the disappearance of the first crystallization peak and the shift of the second crystallization peak to a lower temperature.

Fig. 9 shows XRD patterns for the as-prepared glass together with diffraction patterns obtained after annealing at selected temperatures of 362.5 and 773 K. Fig. 9(a) confirming the glassy (amorphous) nature of the prepared glass. The pattern of the sample annealed at 362 K for 2 h (Fig. 9b) shows Bragg peaks of SSe_{20} phase [19]. Two crystalline phases after fully crystallization after annealing at 773 K for 24 h can be observed in Fig. 9c, i.e., SSe_{20} and Cu_2Se (as a minor phase). These results indicated that the first and second peaks observed in the DSC curve are associated with the crystallization of SSe_{20} and Cu_2Se phases [1], respectively.

Numerous efforts have been realized in order to understand the nature of the glass transition and to relate the value of T_g to easily measurable quantities. One of the best-known relationships is the "two-third" rule proposed by Kauzmann, stating that T_g scales with the melting temperature as $T_g \approx (2/3)T_m$ [20]. This rule is valid for annealed glass at 362.5 K for 2 h with a value of T_g = 315.8 K while not valid for the as-prepared DSC-curve. Following the modified Gibbs–Dimarzio [21] equation, T_g is written as:

$$T_g = \frac{T_0}{1 - \beta(< r > -2)} \tag{7}$$

where T_0 is the glass transition temperature of the chain-like glass (e.g. vitreous selenium with T_0 = 316 K), for a two component glass AB (e.g. Cu_2Se), β is given by [22]:

$$\frac{1}{\beta} = (m_B - 1)\ln\frac{m_B}{2} \tag{8}$$

where m_B is the number of valencies of atom B. It is found that β = 0.72 for Cu_2Se and the average coordination number $\langle r\rangle$ is defined in a M-component glass by $\langle r\rangle = \sum_{i=1}^{M} m_i x_i$, where m_i is the valence of an atom with concentration x_i. The calculated

value of $\langle r \rangle$ for Cu_2Se is 2 and consequently the calculated T_g is found to be 316 K. Therefore, the glass transition temperature, T_g associated with the annealing exothermic peak belongs to the Cu_2Se phase. The T_g broadened endothermic peak in Fig. 1 is consists of two overlapping peaks, one for SSe_{20} phase and the other for Cu_2Se phase.

The activation energies to be considered in a crystallization process are the activation energy for nucleation (E_n), activation energy for crystal growth (E_G) and that for the whole process of crystallization, called the activation energy for crystallization denoted by E_c. The thermal analysis methods enable the determination of E_c [1,23–26]. It has been pointed out [27] that in non-isothermal measurements, generally due to a rapid temperature rise and big differences in the latent heats of nucleation and growth, the crystallization exotherm characterizes the growth of the crystalline phase from the amorphous matrix; nucleation is more or less calorimetrically unobservable at temperatures below the crystallization exotherm, or it takes place very rapidly and immediately after overheating of the material in the initial stages of the crystallization exotherm, which results in the deformed beginning of the measured exotherm. consequently, the obtained values of E_c can be taken to represent the activation energy of growth, E_G of this $Cu_{0.3}(SSe_{20})_{0.7}$ chalcogenide glass.

4. Conclusions

The glass transition behavior and crystallization kinetics of $Cu_{0.3}(SSe_{20})_{0.7}$ chalcogenide glass have been investigated by non-isothermal DSC and XRD. The $Cu_{0.3}(SSe_{20})_{0.7}$ chalcogenide glass exhibits two crystallization exotherms corresponding to the formation of SSe_{20} and Cu_2Se. The activation energies for glass transition temperature and crystallization phenomena were calculated. It is seen that the activation energy of the first crystallization peak is lower than that of the second peak. This study clearly confirms and emphasizes the importance of a prior knowledge of the crystallization mechanism before being able to apply non-isothermal analyzes in a meaningful manner.

References

[1] A.A. Soliman, Thermochim. Acta 423 (2004) 71.
[2] J. Vázquez, P.L. López-Alemany, P. Villares, R. Jiménez-Garay, J. Alloys Compd. 354 (2003) 153.
[3] A.A. Soliman, to be published.
[4] W.H. Wang, Y.X. Zhuang, M.P. Xiang, Y.S. Yao, J. Appl. Phys. 88 (2000) 3914.
[5] P.F. Xing, Y.X. Zhuang, J. Appl. Phys. 91 (2002) 4956.
[6] R.A. Ligero, J. Vázquez, M. Cases-Ruiz, R. Jimenez-Garay, Thermochim. Acta 197 (1992) 319.
[7] C. Wagner, P. Villares, J. Vázquez, R. Jimenez-Garay, Mater. Lett. 15 (1993) 370.
[8] J. Vázquez, C. Wagner, P. Villares, R. Jimenez-Garay, Acta Mater. 44 (1996) 4807.
[9] C.T. Moynihan, A.J. Eastel, J. Wilder, J. Tucker, J. Phys. Chem. 78 (1974) 2673.
[10] C.T. Moynihan, S.-K. Lee, M. Tatsumisago, T. Minami, Thermochim. Acta 153 (1996) 280.
[11] S. Vyazovkin, N. Sbirrazzuoli, I. Dranca, Macromol. Rapid Commun. 25 (2004) 1708.
[12] T.M. Lasocka, Mater. Sci. Eng. 23 (1976) 173.
[13] H.E. Kissinger, J. Res. Natl. Bur. Stand. 57 (1956) 217.
[14] K. Matusita, T. Konatsu, R. Yorota, J. Mater. Sci. 19 (1979) 81.
[15] K. Matusita, S. Sakka, Thermochim. Acta 33 (1979) 351.
[16] J. Colemenero, J.M. Barandiaran, J. Non-Cryst. Solids 30 (1978) 263.
[17] A. Morotta, S. Saiello, A. Buri, J. Non-Cryst. Solids 57 (1983) 473.
[18] K. Matusita, S. Sakka, J. Non-Cryst. Solids 38–39 (1980) 741.
[19] Z.K. Heiba, M.B. El-Den, K. El-Sayed, Powder Diffr. 71 (2002) 191.
[20] W. Kauzmann, Chem. Rev. 43 (1948) 219.
[21] J.H. Gibbs, E.A. Dimarzio, J. Chem. Phys. 28 (1958) 373.
[22] R. Kerner, M. Micoulaut, J. Non-Cryst. Solids 210 (1997) 298.
[23] S. Ranganathan, M. von Heimendahl, J. Mater. Sci. 16 (1981) 2401.
[24] M. von Heimendahl, G. Kuglstatter, J. Mater. Sci. 16 (1981) 2405.
[25] A.A. Soliman, S. Al-Heniti, A. Al-Hajry, M. Al-Assiri, G. Al-Barakati, Thermochim. Acta 413 (2004) 57.
[26] A. Al-Hajry, A.A. Soliman, M.M. El-Desoky, Thermochim. Acta 427 (2005) 181.
[27] E. Illekova, J. Non-Cryst. Solids 68 (1984) 153.